NASA/TM—2001-210977 AIAA–2001–2521

Ten Years in the Making—AUSM-family

Meng-Sing Liou
Glenn Research Center, Cleveland, Ohio

Prepared for the
15th Computational Fluid Dynamics Conference
sponsored by the American Institute of Aeronautics and Astronautics
Anaheim, California, June 11–14, 2001

National Aeronautics and
Space Administration

Glenn Research Center

November 2001

Acknowledgments

Several people have kindly permitted and sent me their calculated results that are included in the present paper. Thanks are due to Drs. G. Billet and I. Mary of ONERA, France, D. Darracq of CERFACS, France, H. Paillère of CEA, France, and J. De Wilde of University of Ghent, Belgium. Dr. Y. Zheng of Taitech, Inc. helped in the preparation of the manuscript.

Available from

NASA Center for Aerospace Information
7121 Standard Drive
Hanover, MD 21076

National Technical Information Service
5285 Port Royal Road
Springfield, VA 22100

Available electronically at http://gltrs.grc.nasa.gov/GLTRS

Ten Years in the Making – AUSM-family

Meng-Sing Liou
National Aeronautics and Space Administration
Glenn Research Center
21000 Brookpark Road
Cleveland, Ohio 44135

We begin by describing the motivations that gave birth to the original AUSM scheme and then focus on the ingredients that has spurred its growth and acceptance by the world of computational fluid dynamics. As it has played out more in the field, weaknesses have also surfaced. Hence, nutrients and supplements are prescribed to help it grow and stay strong and robust. In this paper, We will describe the saga of efforts owing to researchers who have contributed to building up the AUSM-family for the CFD community. It is hoped that a healthy scheme will contribute to the accurate and robust solution of problems encountered in a wide range of disciplines. We analyze numerical mass fluxes with an emphasis on their capability for accurately capturing shock and contact discontinuities. We will present a new scheme for the pressure flux, along with results for a host of test problems.

Introduction

CONSIDERABLE progress in CFD has been made in solving equations of conservation laws over the last two decades, particularly in devising *accurate* and *robust* schemes for capturing *shock* and *contact* discontinuities. The ability to predict shock and contact discontinuities can be considered a prerequisite for a reliable and accurate solution to both inviscid and viscous problems. The 1980s witnessed an explosive interest and research in upwind schemes for their capability of achieving high accuracy over a wide range of problems described by Euler or Navier-Stokes equations. Today, upwind schemes undoubtedly have become the main spatial discretization techniques adopted into nearly all major research and commercial codes. Yet some deficiencies or failures have been experienced by some upwind schemes, such as shock instability in multidimensions, creation of traveling waves in slowly moving shock,[1] and violation of positivity-preserving.[2] As CFD is being used more routinely and extended to more complicated systems of flow equations, the need for maximizing accuracy, efficiency and robustness for a wide variety of problems still remains the foremost concerns. Hence, the quest for the ultimate numerical flux scheme continues.

Since the inception of the AUSM scheme in 1990,[3] it has been adopted by researchers worldwide. It has been proven to be accurate, simple, robust, and easy to extend to other types of conservation laws, thus providing an attractive alternative to the existing schemes. In spite of the enormous progress achieved, deficiencies have been experienced, typically the post-shock overshoots and pressure oscillations along the transverse direction in the boundary layers, as summarized previously.[4] Several attempts have been made over the last ten years, e.g., Refs.[1,4–10] to improve the original scheme[3] and in general, some successes have been achieved. Now various versions of the AUSM-family schemes have been incorporated into both research and commercial codes. In this paper, we will show some of those results, including low Mach number flows, multiphase flows, and DNS calculations.

As evident in this paper and others, the numerical inviscid flux (which for the sake of simplicity we will hereafter refer to as numerical flux) plays a central role in effecting the success of a calculation, especially with regard to robustness and accuracy. Furthermore, we show in Ref. 2 that the mass flux plays the central role in the construction of a robust and accurate numerical flux that is simultaneously free of anomalies such as the odd-even decoupling and "carbuncle" phenomena. This become clear by realizing that the mass flux is common to the convective part of every conservation equation of the fluid flows.

This paper is organized as follows. First, we will take a broad approach to constructing the AUSM schemes, beyond the original one. We will examine in turn the mass flux and the pressure flux. Next, we will present the recently-introduced concept of a numerical speed of sound, which allows for a unified formula valid for the entire speed regime. It also lends itself conveniently to the extension of the schemes to deal with multiphase/multifluid flows. Examples of applying the AUSM-family schemes to various types of flows will be shown. Finally, we will propose a further development in regard to pressure flux, along with validation tests to demonstrate its effectiveness.

Equations of Conservation Laws

A set of equations of general conservation laws is considered:

$$\mathbf{Q}_t^{(k)} + \mathrm{div}(\vec{\mathbf{F}}^{(k)} + \vec{\mathbf{F}}_{\mathrm{v}}^{(k)}) = \mathbf{S}. \tag{1}$$

We will denote by an overhead arrow " $\vec{}$ " the vectors associated with the Cartesian coordinates in three dimensions. The conservative variables are given in $\mathbf{Q}^{(k)}$ where the superscript $k(=1,2,...)$ is introduced to include multifluid models, often adopted for describing multiphase flows.[11,12] The inviscid and viscous fluxes are denoted respectively by $\mathbf{F}^{(k)}$ and $\mathbf{F}_{\mathrm{v}}{}^{(k)}$, whose definitions are omitted herein since they are rather standard. However, the source terms are dependent upon the physical problems studied. For multiphase flows, they can contain terms describing interfacial balances of mass, momentum, and energy transfers due to phase differences/changes. We include this option because examples will be given later in the paper.

During the 90s, a great deal of interest has been focused upon the development of a (local) preconditioning method to improve the convergence rate in the low Mach number regime. This is accomplished by premultiplying the time-derivative term with a conditioning matrix $\mathbf{\Gamma}$.

$$\mathbf{\Gamma}\dot{\mathbf{Q}}_t^{(k)} + \mathrm{div}(\vec{\mathbf{F}}^{(k)} + \vec{\mathbf{F}}_{(\mathrm{v})}^{(k)}) = \mathbf{S}, \quad \dot{\mathbf{Q}}^{(k)} = (p_k, \vec{V}_k, T_k)^T. \tag{2}$$

Several forms of the local preconditioning matrix $\mathbf{\Gamma}$ have been proposed in the literature, e.g., Refs. 13–16.

The discretization of viscous terms is rather standard and is generally done with centered schemes. On the other hand, treatment of the source terms varies considerably and this subject is not so easy because it is quite problem-dependent and the terms can be extremely complicated. See for example the ones involved in the fluidized bed.[17] The subject is beyond the scope of this paper and will not be dealt with here. We shall restrict ourselves instead to the numerical representation of inviscid fluxes, which has been a subject of intensive effort by many researchers over the past three decades.

Numerical Flux: AUSM-Family

How It Began

The 80s saw the rise of two classes of upwind schemes, namely the flux-vector and flux-difference schemes. The van Leer scheme belongs to the former and is perhaps the most robust one among all for the Euler equations, aside from a slight disadvantage in the shock resolution compared to the latter. Especially, it endures the positivity test and is free from shock instabilities, in addition to its algorithmic simplicity and generality. Interestingly, these properties served well during the era of revived interest in the hypersonic flight, e.g., the NASP program in the US and similar programs in the other countries. As more confidence has been gained by the CFD community in dealing with complexities in flow fields as well as in geometries, CFD has flourished and naturally Navier-Stokes solutions now have taken the center stage. The paper by Van Leer et al.[18] points out that the flux-vector schemes are diffusive for the Navier-Stokes calculations, as illustrated in the 1D conical viscous flow where an incorrect wall temperature was predicted along with a thicker boundary layer. See Fig. (1a). This spelt the downfall of the flux-vector schemes.

In an attempt to resuscitate his scheme for the 90s, Van Leer injected the flavor of flux-difference splitting, as first suggested by Hänel and Schwane,[19] in the CFD symposium held at NASA Lewis Center in 1990.[1] The improvement due to this new idea is clearly demonstrated in Fig. (1b), showing the wall temperature close to the correct value of 13.7 ($Pr = 1.0$), but unfortunately afflicted with pressure irregularity at the edge of the boundary layer. It appeared that the flux-vector scheme was a phoenix, the catalyst for its rebirth being the combination with flux-splitting scheme. So Van Leer asked the question: Can pure flux-vector splitting be saved? The key word is "pure" and the answer may be still up in the air. But the question can be rephrased as: Can the Van Leer splitting be engineered so that good "genes" are kept? The answer is very likely. Hence, research started and the original AUSM scheme[3] (presented in this conference the first time in 1991[20]) began to take shape. As a result of this quest, the AUSM scheme gives the temperature profile in excellent agreement with the solution by the Godunov scheme.[21]

How it is shaping up

In this section, we will look at the algorithm involved in the AUSM-family schemes and the new developments. For more details and other numerical properties, the reader should consult with the cited references.

As a first step common in the AUSM schemes, we explicitly split the inviscid flux (written in three dimensions) into two parts:

$$\vec{\mathbf{F}} = \vec{\mathbf{F}}^{(c)} + \vec{\mathbf{P}} = \vec{\dot{m}}\psi + \vec{\mathbf{P}}, \tag{3}$$

where

$$\vec{\dot{m}} = \rho\vec{V}, \quad \psi = (1, u, v, w, H)^T, \quad \vec{\mathbf{P}} = (0, p\vec{i}, p\vec{j}, p\vec{k}, 0)^T. \tag{4}$$

[1] This occasion brought together the fathers of two flux-vector splittings, Joe Steger and Bram van Leer, although Joe talked about an entirely different subject–the chimera method. My family and I had a great deal of fun with them in my home that evening; the fun of course was heightened with Bram's playing piano, especially performing Joe's favorite piano and orchestral piece, Symphonic Variations by Cesar Franck.

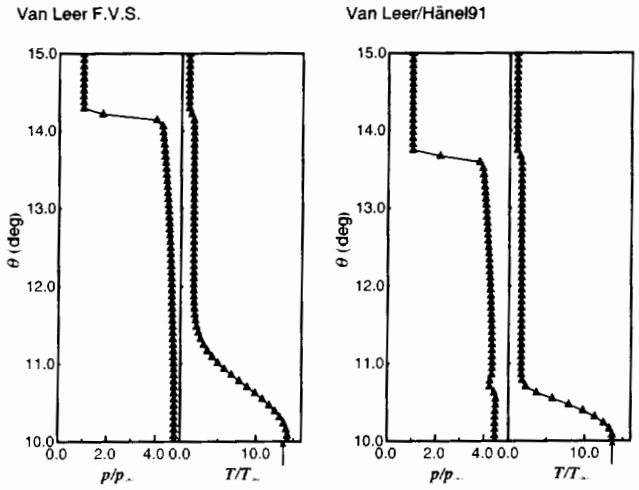

a) Van Leer FVS. b) Van Leer/Hänel ('90).

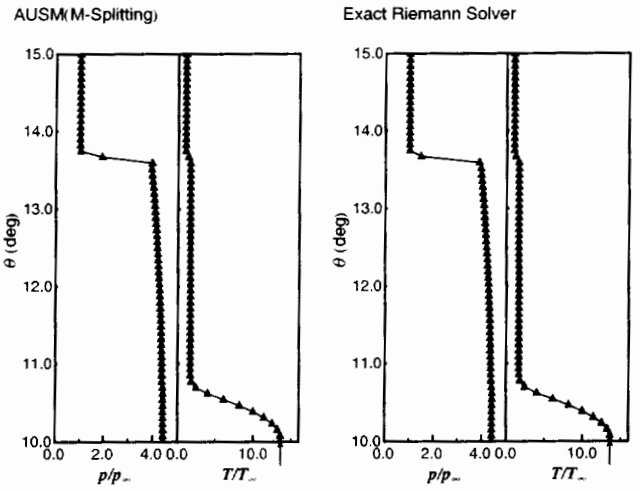

c) AUSM ('91). d) Godunov Riemann solver.

Fig. 1 Hypersonic conic flow, $M_\infty = 7.95, \theta_{\text{cone}/2} = 10^o$ and $Re_\infty = 4.2 \times 10^5$.

The first term in $\vec{\mathbf{F}}$ is the *convective* flux $\vec{\mathbf{F}}^{(c)}$, indicating the convection of ψ by the mass flux $\vec{\dot{m}}$ and the second term is the *pressure* flux $\vec{\mathbf{P}}$, containing nothing but the pressure. It is noted that the conservation of the total enthalpy is guaranteed if H, instead of total internal energy (E), is contained in ψ. Halt and Agarwal[22] split H into E and p/ρ and put them respectively in the ψ and $\vec{\mathbf{P}}$ terms and called it the WPS scheme.

In terms of the component fluxes in the directions of x, y, and z, we have

$$\vec{\mathbf{F}} = (\dot{m}_x\psi + \mathbf{P}_x)\vec{i} + (\dot{m}_y\psi + \mathbf{P}_y)\vec{j} + (\dot{m}_z\psi + \mathbf{P}_z)\vec{k}. \quad (5)$$

where

$$m_l = \rho u_l, \quad \mathbf{P}_l = (0, p\delta_{lx}, p\delta_{ly}, p\delta_{lz}, 0)^T, \quad l = x, y, z. \quad (6)$$

In a control volume, the mass flux $\dot{m}_n$ through a control surface element having a unit normal vector $\vec{n} = (n_x, n_y, n_z)$ is given by

$$\dot{m}_n = \rho\vec{V}\cdot\vec{n} = n_x\,\dot{m}_x + n_y\,\dot{m}_y + n_z\,\dot{m}_z\,. \quad (7)$$

And the associated flux becomes,

$$\mathbf{F}_n = \dot{m}_n\,\psi + \mathbf{P}_n, \quad \mathbf{P}_n = p(0, n_x, n_y, n_z, 0)^T. \quad (8)$$

Formally, this equation looks the same as that along an individual Cartesian coordinate direction. Hence, at each control surface, the mass flux is treated in an one-dimensional fashion. At the discrete level, this is also what one needs to do for defining the flux at the interface in a finite volume. Hereafter, we will assume that this local orientation has been accomplished and the velocity vector (hence mass flux) has been decomposed into components normal and parallel to the surface vectors $\vec{n}$. Therefore, the subscript "n" denoting the normal component will be dropped.

From the above equations, the principal quantities in $\mathbf{F}_n$ are again the convective flux and the pressure flux. The distinction of these two fluxes gives rise to the basis for the development of the AUSM-family schemes. Since the mass flux appears in all equations, its effects will be felt by all the variables. Hence, we believe that it is desirable to observe this fact at the discrete level as well when devising a new scheme. Significant benefits can be derived as well. For example, the numerical dissipation term is scalar even for the system of equations; it is just as easy to add more conservation equations insofar as the numerical flux is concerned.

It is possible to write a numerical flux, mimicking the expression at the continuum level, in terms of a common mass flux in the following general upwind form.

$$\begin{aligned}\mathbf{f}_{1/2} &= \dot{m}_{1/2}\,\psi_{L/R} + \mathbf{p}_{1/2} \\ &= \dot{m}^+_{1/2}\psi_L + \dot{m}^-_{1/2}\psi_R + \mathbf{p}_{1/2}.\end{aligned} \quad (9)$$

Here the contributions of ψ_L and ψ_R are weighted by the split masses $(\dot{m}^+_{1/2}, \dot{m}^-_{1/2})$, which must follow the consistency requirement,

$$\dot{m}_{1/2} = \dot{m}^+_{1/2} + \dot{m}^-_{1/2}\,. \quad (10)$$

This fact is automatically satisfied by the first element of $\mathbf{f}$. One can rewrite Eq. (9), using Eq. (10), as

$$\mathbf{f}_{1/2} = \frac{1}{2}\,\dot{m}_{1/2}\,(\psi_L + \psi_R) - \frac{1}{2}\mathcal{D}_m(\psi_R - \psi_L) + \mathbf{p}_{1/2}, \quad (11)$$

The dissipation term, $\mathcal{D}_m$, is

$$\mathcal{D}_m = \dot{m}^+_{1/2} - \dot{m}^-_{1/2}\,. \quad (12)$$

The subscripts "L" and "R" are understood to mean the cell centers on either side of the interface at which

the normal vector is assumed to point from "L" to "R".

The quantities $(\overset{\bullet}{m}^{+}_{1/2}, \overset{\bullet}{m}^{-}_{1/2})$ are required to satisfy these conditions,

$$(\overset{\bullet}{m}^{+}_{1/2}) \geq 0, \quad (\overset{\bullet}{m}^{-}_{1/2}) \leq 0, \tag{13}$$

so that they provide proper upwinding, thus ensuring stability. In the AUSM-family schemes, these two variables are mutually exclusive, i.e.,

$$(\overset{\bullet}{m}^{+}_{1/2})\ (\overset{\bullet}{m}^{-}_{1/2}) \equiv 0, \tag{14}$$

It must be noted that the flux expressed in the form of Eq. (9) implies that the numerical dissipation is of the scalar, rather than the matrix form, because the same factors $\overset{\bullet}{m}^{+}_{1/2}$ are applied throughout for all conservation equations. The flux difference splitting schemes are known to belong to the category of matrix dissipation. On the other hand, the category of scalar dissipation encompasses several existing schemes other than the AUSM-family schemes, such as central differencing with artificial damping, the Van Leer flux vector scheme, the HLLE scheme. Indeed, there are several attractive properties associated with the scalar form of dissipation. From the algorithmic viewpoint, it offers simplicity, efficiency, and generality allowing for an easy extension to other systems of equations.

The 1991 AUSM scheme has served well by laying out the basis for further developments. One of the important developments is the concept of common speed of sound, which makes an accurate resolution of contact and shock discontinuities possible for both steady and unsteady flows. As a result, two new members of the AUSM-family were generated, We shall in this paper, specifically concentrate on a unified formulation encompassing both the AUSM$^+$ and AUSMDV schemes.

In what follows, we will give some basic formulas used to define the mass flux. To facilitate the discussion, we first define the following split functions.

$$\begin{aligned} \mathcal{M}^{\pm}_{(1)}(M) &= \tfrac{1}{2}(M \pm |M|), \\ \mathcal{M}^{\pm}_{(2)}(M) &= \pm\tfrac{1}{4}(M \pm 1)^2 \end{aligned} \tag{15}$$

$$\mathcal{M}^{\pm}_{(4)}(M) = \begin{cases} \mathcal{M}^{\pm}_{(1)}(M), & \text{if } |M| \geq 1, \\ \mathcal{M}^{\pm}_{(2)}(1 \mp 2\mathcal{M}^{\mp}_{(2)}), & \text{otherwise}, \end{cases} \tag{16}$$

and

$$\mathcal{P}_{(5)}{}^{\pm}(M) = \begin{cases} \frac{1}{M}\mathcal{M}^{\pm}_{(1)}(M), & \text{if } |M| \geq 1, \\ \mathcal{M}^{\pm}_{(2)}[(\pm 2 - M) \mp 3M\mathcal{M}^{\mp}_{(2)}], & \text{otherwise}. \end{cases} \tag{17}$$

The numerals in the subscript of $\mathcal{M}^{\pm}_{(1)}, \mathcal{M}^{\pm}_{(2)}, \mathcal{M}^{\pm}_{(4)}$, and $\mathcal{P}^{\pm}_{(5)}$ indicate the degree of polynomials.

Using a common speed of sound $a_{1/2}$ to define $M_L = u_{n_L}/a_{1/2}$ and $M_R = u_{n_R}/a_{1/2}$.

For the AUSM$^+$: we first define the interface Mach number

$$M_{1/2} = \mathcal{M}^{+}_{(4)}(M_L) + \mathcal{M}^{-}_{(4)}(M_R), \tag{18}$$

then

$$M^{\pm}_{1/2} = \frac{1}{2}(M_{1/2} \pm |M_{1/2}|). \tag{19}$$

Now for the AUSMDV: we first define the interface split Mach numbers,

$$M^{\pm}_{1/2} = \left[\omega^{\pm}_{1/2}\mathcal{M}^{+}_{(2)}(M_{L/R}) + (1 - \omega^{\pm}_{1/2})\mathcal{M}^{+}_{(1)}(M_{L/R})\right], \tag{20}$$

together with the blending functions,

$$\omega^{+}_{1/2} = \frac{2f_{L/R}}{f_L + f_R}, \quad f = p/\rho. \tag{21}$$

Then, the interface Mach number is

$$M_{1/2} = M^{+}_{1/2} + M^{-}_{1/2}. \tag{22}$$

It is noted that the construction of the interface split Mach numbers $M^{\pm}_{1/2}$ in the AUSMDV scheme is somewhat similar to that in the Van Leer's flux scheme, one might then wonder if the AUSMDV would be also afflicted with the same shortcomings. To the credits of the variables, $\omega^{\pm}$ varying with flow variables, they make AUSMDV an accurate scheme for capturing contact discontinuities, hence appropriate for viscous solutions.

We stress again that a common speed of sound $a_{1/2} = a(\mathbf{U}_L, \mathbf{U}_R)$ is used in the formulation in defining the "L" and "R" Mach numbers and in Eq. (9). In Ref. 6, we give a special formula for $a_{1/2}$ so that an exact capturing of a stationary normal shock is achieved. Otherwise, any averages of the "L" and "R" states should be appropriate. More importantly, this possibility of flexibly allowing other definitions of the common speed of sound opens a very rewarding opportunity, as will be discussed later.

Now the mass flux is immediately available by using the quantities $M^{\pm}_{1/2}$:

$$\begin{aligned} \overset{\bullet}{m} &= a_{1/2}(\rho_L M^{+}_{1/2} + \rho_R M^{-}_{1/2}) \\ &= \tfrac{1}{2}a_{1/2}[M_{1/2}(\rho_L + \rho_R) - D_\rho(\rho_R - \rho_L)] \end{aligned} \tag{23}$$

We remark that a clear difference between the AUSMDV and AUSM$^+$ schemes, insofar as $\overset{\bullet}{m}$ is concerned, is in the definition of $M^{\pm}_{1/2}$.

It is easy to show that:

$$D_\rho = \begin{cases} |M_{1/2}| & \text{AUSM}^+ \\ M^{+}_{1/2} - M^{-}_{1/2} & \text{AUSMDV} \end{cases} \tag{24}$$

and

$$M^{+}_{1/2}M^{-}_{1/2} \begin{cases} \equiv 0 & \text{AUSM}^+ \\ \leq 0 & \text{AUSMDV} \end{cases} \tag{25}$$

The dissipation coefficient in the convective flux, in Eq. (11), is now explicitly given as

$$\mathcal{D}_m = |\, \dot{m}_{1/2} \,| \tag{26}$$

We can also rewrite the mass flux in the most general form,

$$\dot{m}_{1/2} = \langle \dot{m} \rangle - \frac{1}{2}\mathcal{D}(\mathbf{U}_L, \mathbf{U}_R). \tag{27}$$

where $\langle \dot{m} \rangle$ is a sort of centrally weighted average, but the detail is not important for our discussion. However, we shall focus on the dissipative term $\mathcal{D}(\mathbf{U}_L, \mathbf{U}_R)$ which can be further expanded in terms of differences of primitive variables $\mathbf{U} = (\rho, \vec{V}, p)^T$ as follows.

$$\mathcal{D} = \mathcal{D}^{(\rho)}(\overline{\mathbf{U}})\Delta\rho + \sum_l \mathcal{D}^{(u_l)}(\overline{\mathbf{U}})\Delta u_l + \mathcal{D}^{(p)}(\overline{\mathbf{U}})\Delta p, \tag{28}$$

where $\overline{\mathbf{U}}(\mathbf{U}_L, \mathbf{U}_R)$ are some mean quantities, and the difference operator is $\Delta(\bullet) = (\bullet)_R - (\bullet)_L$.

It is shown in Ref. 2 that the fact whether the pressure dissipation coefficient $\mathcal{D}^{(p)}$ vanishes for all conditions plays a decisive role in determining the occurrence of the anomalies in shock instabilities.

Finally, another important variable is the pressure flux, which may be written as

$$\mathbf{p}_{1/2} = p_{1/2}(0, n_x, n_y, n_z, 0)^T. \tag{29}$$

Clearly, all one needs in the pressure flux $\mathbf{p}_{1/2}$ is simply the definition of $p_{1/2}$.

In all the AUSM-family schemes, the interface pressure has been simply given by

$$p_{1/2} = \mathcal{P}^+_{(5)}(M_L)p_L + \mathcal{P}^-_{(5)}(M_R)p_R. \tag{30}$$

As simple as it may seem, there apparently are enough opportunities to further enhance the AUSM-family. A new version of the pressure flux will be presented later.

The accuracy of the AUSM$^+$ scheme was thoroughly established by Darracq et al. in Ref. 23 in which they have done studies of grid refinement and spatial order of accuracy for several airfoil flows, against the measured data. Tables 1 and 2 present the comparisons of calculated results for 2D and 3D turbulent flows. They concluded that "for all runs the AUSM$^+$ predictions agree better with the experimental data than results obtained with the Roe scheme." In general, the differences between predictions from these two schemes become more apparent in the prediction of flows near the leading edge on the suction side. It also shows that AUSM$^+$ solutions converge to the grid independent solution faster than those of the Roe splitting.

These results, along with those from my own and others, seem to suggest that the AUSM schemes (especially AUSM$^+$ and AUSMDV) yield little numerical dissipation. Hence attempts have been made recently for simulations touted as demanding high accuracy, such as Large Eddy Simulation (LES), and Direct Numerical Simulation (DNS).

Table 1 Comparison of lift and drag coefficients for the RAE-2822 airfoil, M_∞=0.73, α=2.79°, Re_∞ = 6.5 × 10^6,Baldwin-Lomax model. (Ref. 23)

Scheme	Order	Mesh	C_L	C_{Dp}	C_{Dtot}
Roe	2nd	coarse	0.7755	0.0153	0.0209
AUSM$^+$	2nd	coarse	0.7931	0.0144	0.0200
Roe	3rd	coarse	0.7814	0.0136	0.0192
AUSM$^+$	3rd	coarse	0.7961	0.0133	0.0188
Roe	2nd	fine	0.7916	0.0133	0.0189
AUSM$^+$	2nd	fine	0.8046	0.0132	0.0187
Roe	3rd	fine	0.7927	0.0131	0.0187
AUSM$^+$	3rd	fine	0.8064	0.0131	0.0187
Expt.[24]			0.803		0.0168

Table 2 Comparison of lift and drag coefficients for the ONERA-M6 airfoil, M_∞=0.84, α=3.06°, Re_∞ = 1.749 × 10^7, Baldwin-Lomax model. (Ref. 23)

Scheme	Order	Mesh	C_L	C_{Dp}	C_{Dtot}
Roe	2nd	coarse	0.2558	0.0168	0.0220
AUSM$^+$	2nd	coarse	0.2655	0.0164	0.0215
Roe	3rd	coarse	0.2604	0.0141	0.0192
AUSM$^+$	3rd	coarse	0.2667	0.0138	0.0189
Roe	2nd	fine	0.2782	0.0137	0.0188
AUSM$^+$	2nd	fine	0.2819	0.0138	0.0188
Roe	3rd	fine	0.2791	0.0132	0.0183
AUSM$^+$	3rd	fine	0.2825	0.0132	0.0182

Recently, Billet and Louedin[25] combined the AUSM scheme with a very interesting adaptive limiter (named triad limiter, φ_{triad}) to gain high accuracy for DNS-type simulations of unsteady flows. The limiter is still built upon the third-order accurate MUSCL formulation, but the accuracy of the results rivals that of the higher-order schemes. Advection of a Taylor vortex is simulated using the AUSM-φ_{triad} scheme.[25] and the velocity and pressure profiles, shown in Fig. 2, are in excellent agreement with those from a sixth-order accurate Hermitian scheme. Also Fig. 3 displays the time development of a 3D mixing layer using the same scheme, showing a nearly identical result as that from the DNS.

Other DNS/LES calculations, for example, can be found in Ref. 26-28. There appears a common strategy in the simulation of low speed flows, insofar as using the AUSM schemes is concerned. That is, the pressure term is modified by replacing it with a simple average of neighboring pressures. This seems to have worked well, giving smooth solutions without even adding numerical dissipations. However, this simple replacement gives rise to a smeared shock when applied to supersonic flows. Nevertheless, what this indicates is that there are still some things to be done in the area of

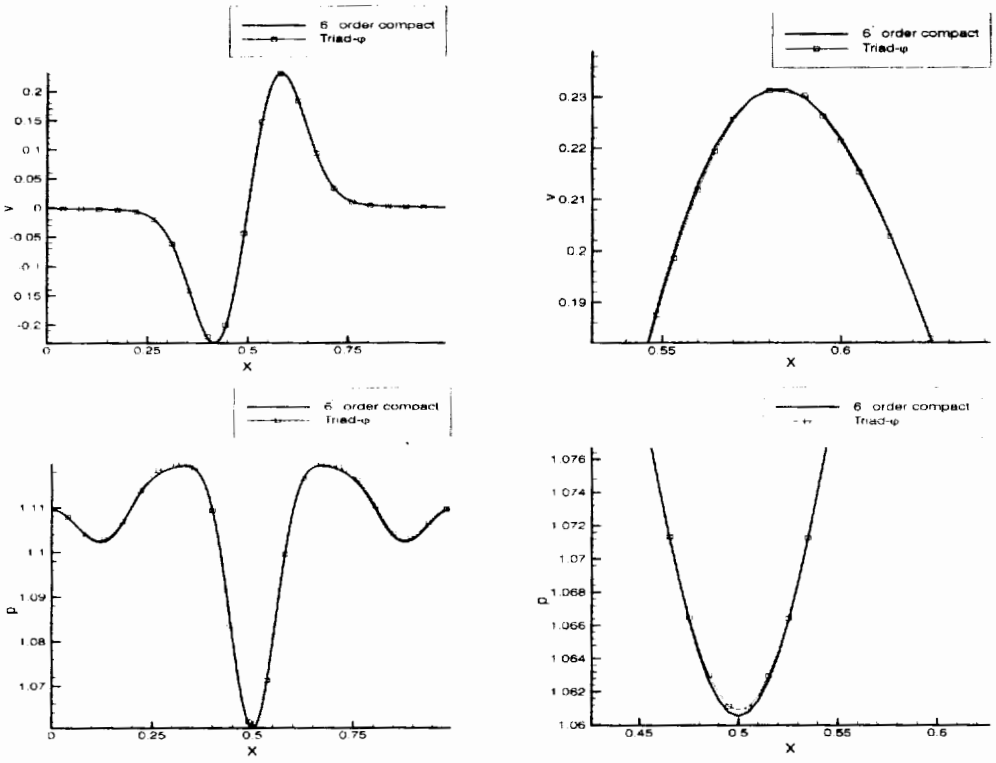

Fig. 2 Taylor vortex advection:longitudinal distribution along the centerline of variables v (top) and p (bottom). The blow-up view near the extrema are shown on the right. (Ref. 25)

pressure splitting. This is the new development yet to be disclosed later in this paper.

In what follows, we will discuss another important chapter about the AUSM family. This is the extension to the low Mach number flows and something other than the aerodynamic flows, for example, multiphase flows.

As it has become known during last decade that the detrimental deficiencies in forcing the compressible upwind codes onto solving low speed flows are : (1) extremely slow or stalled convergence, more so as the flow speed decreases and (2) the flow solutions can be globally incorrect(rather than just locally as in the case of smearing shocks). These two phenomena are not related because the first one originates at the continuum level, depending on the form of governing equations being solved, irrespective of whether the scheme is centered or upwind. However, the second one is inherently tied to the upwind scheme where the eigenvalues, strongly depending on the usage of the speed of sound, are employed.

In the 90s, active research has been conducted to conquer the first problem, in the name of local preconditioning, such as those by Van Leer et al.,[14] Turkel,[13] and Merkle,[15] and their subsequent publications. While there are differences in approaches, they all attempt to achieve the same objectives of making the eigenvalues of the new system of equations, Eq. (2), the same order of magnitude. A condition number κ defined as the largest ratio of eigenvalues,

$$\kappa = \frac{|u| + a}{|u|} \to \infty, \quad \text{as } |u| \to 0, \quad \text{and } a \text{ held fixed.} \tag{31}$$

is a useful measurement. Clearly there is a large disparity of wave speeds as $|u| \to 0$ and as a result this has been identified as the source of slow (or no) convergence.

In the preconditioning strategy, one can think of seeking to modify the system in such a way that the corresponding speed of sound would be altered to behave like $|u|$ as it approaches zero.

Consequently, we will define the numerical speed of sound by

$$\tilde{a} = f(M; M_*)a, \tag{32}$$

where the scaling factor may be of this form,

$$f(M; M_*) = \frac{\sqrt{(1 - M_*^2)^2 M^2 + 4M_*^2}}{1 + M_*^2}, \tag{33}$$

and the reference Mach number,

$$M_*^2 = \min(1, \max(M^2, M_{co}^2)). \tag{34}$$

The cutoff parameter M_{co} is introduced to prevent a singularity at stagnation point. It is a user-specified parameter and $M_{co}^2 = 10^{-4}$ has been used. Details can be found in Ref. 29.

Now the condition number becomes,

$$\kappa_\Gamma = \frac{|u| + \tilde{a}}{|u|} \to O(1), \quad \text{while } \tilde{a} \to 0, \text{ as } |u| \to 0. \tag{35}$$

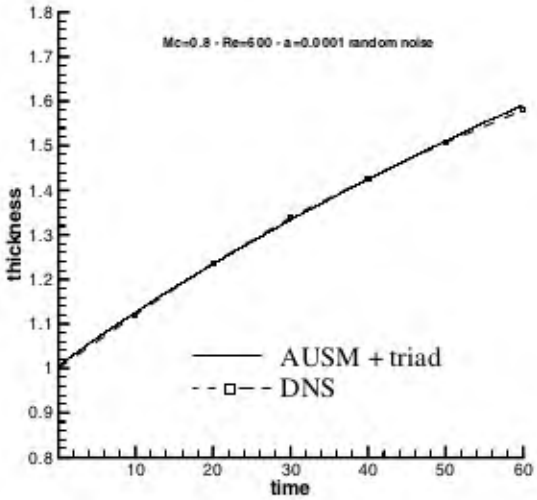

a) Time evolution of vorticity thickness.

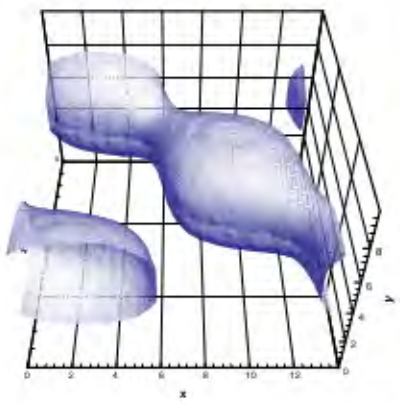

b) One static pressure surface at t=45.

Fig. 3 3D mixing layer. (Ref. 25)

That is, the condition number remains order of unity at low speeds. The numerical dissipation based on this new speed of sound now scales with the local speed $|u|$, instead of the local speed of sound a. As a result, the accuracy can be restored as it is applied to low Mach flows.

Now we can define the new Mach numbers based on this numerical speed of sound $\tilde{a}$ as

$$\tilde{M}_{L/R} = \frac{u_{L/R}}{\tilde{a}} \tag{36}$$

and these would be the entries to the equations for $\mathcal{M}_{(4)}$ and $\mathcal{P}_{(5)}$. This version is then denoted with suffix a, such as AUSM$^+$-a.

Now we show the results performed by Mary et al.[30] using the low Mach number version of the

a) Snapshot of vorticity.

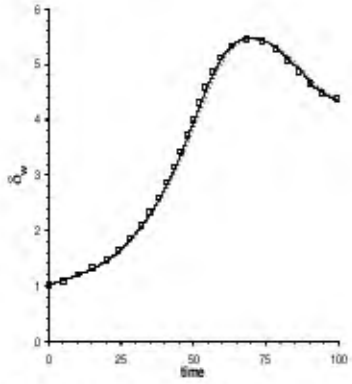

b) Time history of vorticity thickness.

Fig. 4 Comparison of solutions for subsonic compressible mixing layer, third-order accurate solutions of three different time step sizes ($\Delta t = 0.03, 0.06, 0.4$ (shown by ...) are compared on the same number of grid points with that by the sixth-order Hermitian scheme (denoted by □□). Results from two small time steps are indistinguishable. (Ref. 30)

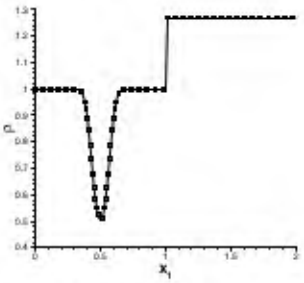

a) Initial setup.

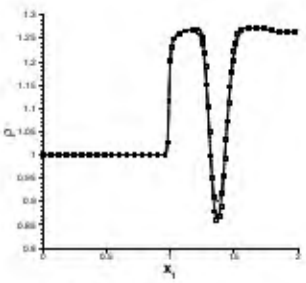

b) After interaction.

Fig. 5 Interaction of a Gaussian temperature spot with a shock. Comparison with the 4th order accurate WENO scheme (denoted by □□) with the 3rd order AUSM$^+$ solutions with three different values of the limiter compression parameter Θ. (Ref. 30)

AUSM$^+$ scheme with a third-order accurate spatial interpolation. Figure. 4 shows that the results of a subsonic compressible mixing layer are in excellent agreement with a sixth-order Hermitian scheme on the same number of grid points, hence demonstrating the accuracy of the AUSM$^+$ scheme. Another example, given in Fig. 5, compares the result with that of the 4th-order accurate WENO scheme for a temperature spot interacting with a shock, again revealing the high accuracy of the AUSM$^+$ scheme.

Implementing AUSM$^+$-a in the code results in a significant improvement not only in solution accuracy, as seen above, but also in convergence rate as well. Another unforeseen but pleasant consequence is that the pressure oscillations, observed along the transverse direction in the viscous layer when using AUSM$^+$ scheme, are no longer there. This results from the fact the much reduced numerical dissipation

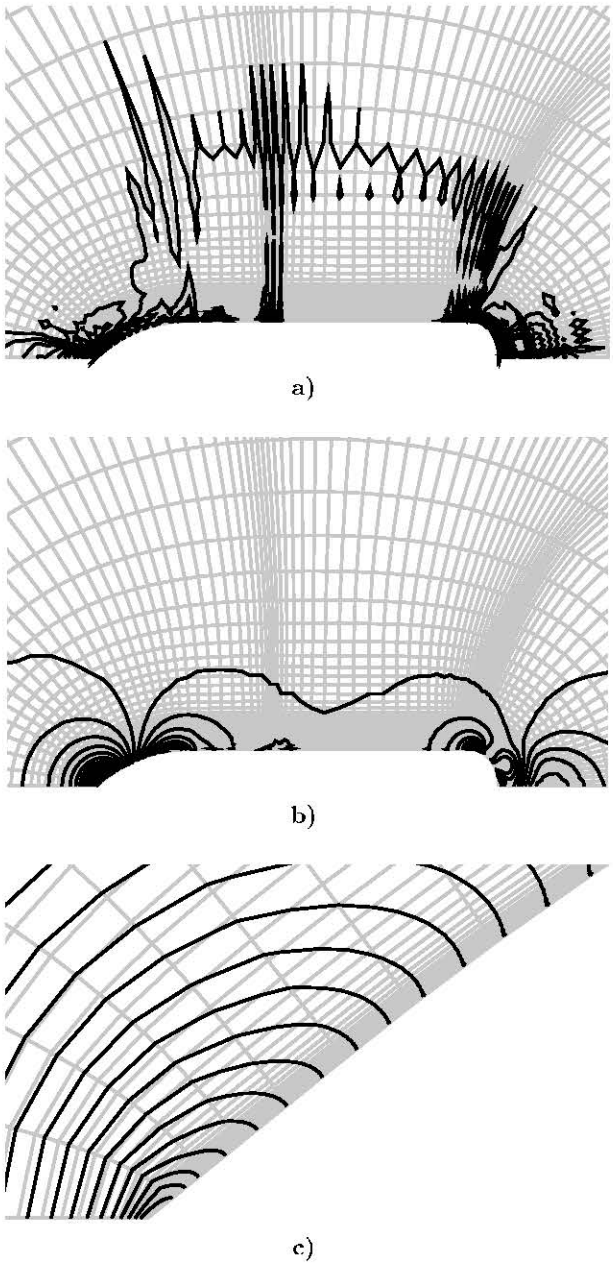

Fig. 6 Pressure contours for the shuttle external tank problem for $M_\infty = 0.01$. a): using the standard AUSM$^+$ at N=6400 time steps; b): using numerical speed of sound at N=1000 time steps, and c): magnified view near the nose.

now scales properly with the pressure variations, as seen in Fig. 6.

Another case in point is the application to a 3D low speed flow over a high-lift three-element trap-wing configuration. The flow conditions are: $M_\infty = 0.1498, Re_\infty = 14.7 \times 10^6$ and angle of attack of 20 degrees. The computational geometry model consists of a body pod, a wing, a full-span slat, a full-span flap and the tunnel walls, as displayed in Fig. 7. Rogers et al. performed an extensive numerical study of the aerodynamic characteristics of this configuration using the preconditioned version of the Roe

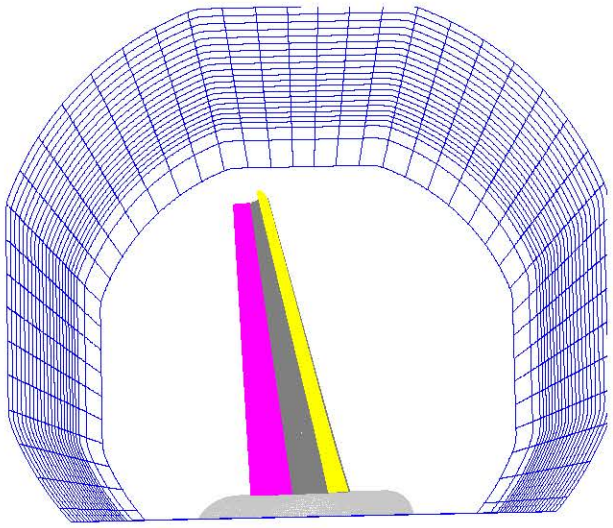

Fig. 7 Trap wing model in a wind tunnel, the tunnel grid is plotted every fourth grid point.

scheme in the OVERFLOW[31] code. The effectiveness of the AUSM$^+$-a scheme was tested for this configuration and details will be given in a separate paper.[32] The calculation[2] was also performed with the OVERFLOW code, with the Spalart-Allmaras one-equation model.[33] The pressure distributions at various spanwise locations are compared with the experimental data in Fig. 8 and they are in excellent agreement.

The vortices generated from the wing tips and the body pod are illustrated with the particle traces displayed in Fig. 9

Recently, the AUSM-family has been extended to the multiphase flow calculations, e.g., in Refs. 34 36. Paillère et al. solved a system of two-fluid models with interfacial source terms included. Several features that are different from the usual equations for aerodynamic flows add complexity significantly. That is, the system is no longer in conservative form because of the presence of the source terms and the system is not guaranteed to be hyperbolic because it admits complex eigenvalues. Figure 10 displays the computed evolution of an initially homogeneous mixture of liquid water and air, under the action of gravity, moving toward a complete phase separation at the final steady state. The phase separation begins at the both ends and gradually migrates towards the center, as illustrated by the evolution of void fraction of the air, with x measured from the top; the pressure at the steady state is essentially constant in the gas region, but increases linearly in the liquid region, as it should. Next, Paillère et al. also obtained results for a water/air column oscillating under the gravity. The solution includes the effect of interfacial drag. The void fraction of air and the time variation of liquid velocity at the

[2]Dr. Stuart Rogers of NASA Ames Research Center, kindly provided the grid, the post-processing code for extracting the surface pressure and consultations.

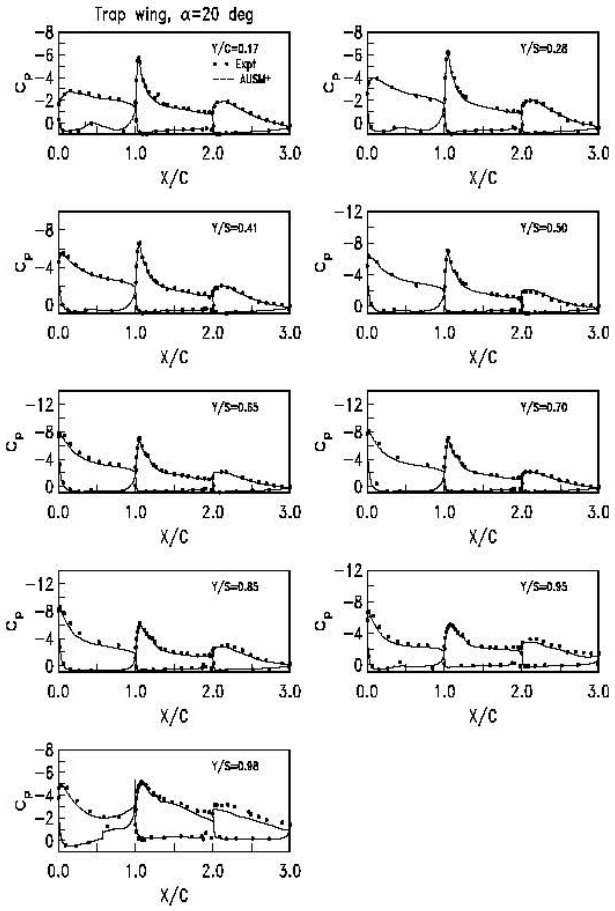

Fig. 8 Pressure distributions.

bottom of the tube are shown in Fig. 11, displaying a cyclic motion. The initially sharp profile of void fraction is now smeared at $t = 20$, due to the interfacial drag.

Another example of multiphase flows involves a water flow over a hemispherical cylinder. The flow can undergo cavitation if the pressure difference (cavitation number, $K = 2(p_\infty - p_v)/\rho_\infty U_\infty^2$) is low enough. Figure 12 shows the water density contours in a turbulent flow under various cavitation conditions. It clearly shows the phase transition between the liquid and vapor states. As K decreases, the pressure in the expansion region drops to the vapor pressure, resulting in the generation of a vapor phase and the growth of a cavitation bubble. Pressure recovery further downstream leads to the collapse of the cavity in a "wake" region. The structure of the wake region is strongly influenced by both the thermodynamic model and the velocity field, which in itself is influenced by the turbulence model.

Another recent accomplishment of using the AUSM scheme has been reported in Ref. 17 by De Wilde et al. for an extremely complicated set of equations and flow patterns involving solid particles and gas phase in an industrial scale riser with a diameter of 1.56 m and a height of 14.434 m. The system is described by an

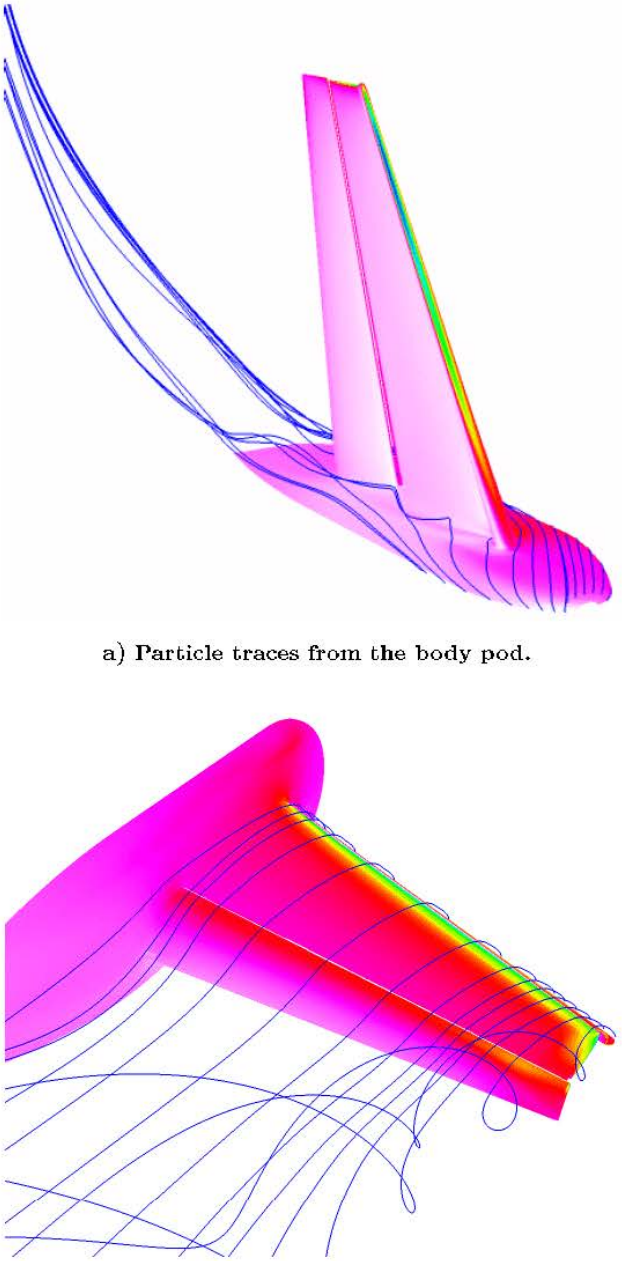

a) Particle traces from the body pod.

b) Particle traces from the wing.

Fig. 9 Particle traces.

unsteady 3D turbulent, two-fluid model. The source terms include gravity, buoyancy, and stresses due to gas-solid interactions. The solid particles along with the gas, entered at velocities of 6.0 and 12.635 (m/s) respectively, in an inlet at the bottom of the riser, and the mixture exited at the top. Due to the inelastic particle-particle collisions, flow instability is triggered and a periodic slugging flow pattern was obtained by them. Figure 14 displays the evolution of solid volume fraction in one cycle. A perturbation is seen to originate at the top of the riser, grow underneath towards the bottom of the riser, and reach the maximum extent at about 3.2 sec and then move upward till it is blown out at the top when t=6.4 sec. Then the cycle contin-

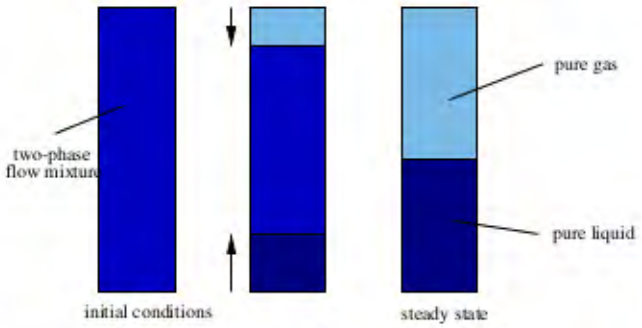

a) Physical description.

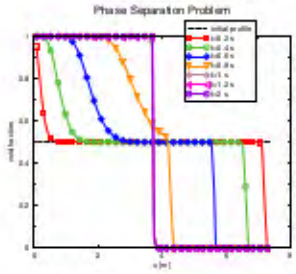

b) Evolution of void fraction to steady state.

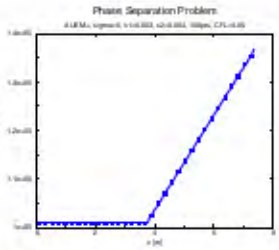

c) Pressure profile at steady state.

Fig. 10 Phase separation test case. (Ref. 34)

ues. From the results, one sees a large scale motion in the axial direction together with a radial variation in each time frame. However, no circumferential asymmetry was found for the conditions calculated. The authors state that the oscillation frequency of 0.15 Hz is in good agreement with that reported in literature. The time-averaged result give distinct boundaries of a cell-like structure.

The above has merely captured representative adventures of the AUSM-family schemes beyond aerodynamics. The DNS/LES calculations demonstrate the accuracy inherent in the AUSM-family schemes, rivaling that of the higher-order schemes. The multiphase flow problems are certainly far more difficult to deal with, not only from the closure (modeling) point of view, but also from the algorithmic one. The source terms strongly couple variables associated with all phases and give rise to an extremely stiff system. Robustness of a numerical scheme is the key to the capability of simulating these types of flows.

To add a contribution for the new millennium, I shall present in what follows the result of a recent effort, with an aim at further improving the scheme's robustness and accuracy. Up to this point, calculating flows at low speeds often required adding a pressure-diffusion term to the mass flux in order to enhance convergence. This has been commonly done in the incompressible code to ensure pressure-velocity coupling. In spite of its effectiveness, it nevertheless stems purely from numerical consideration. So the questions to ask are: (1) whether this (adding the pressure-velocity term) is absolutely necessary? (2) if yes, whether this is the only way? and (3) if not, what then?

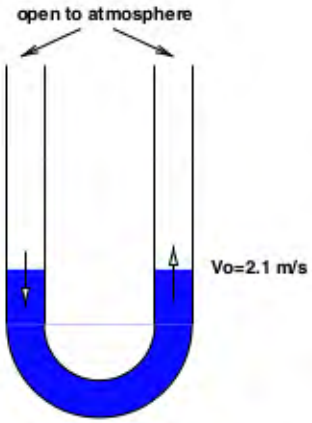

a) Physical setup.

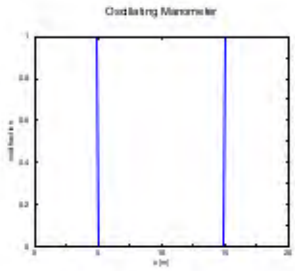

b) Initial conditions.

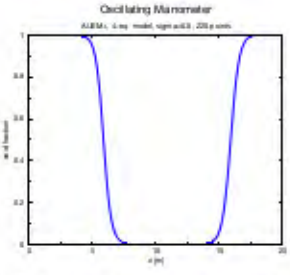

c) Void fraction at t=20 s.

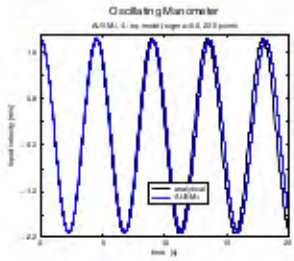

d) Liquid velocity at x=10 m.

Fig. 11 Oscillating manometer. (Ref. 34)

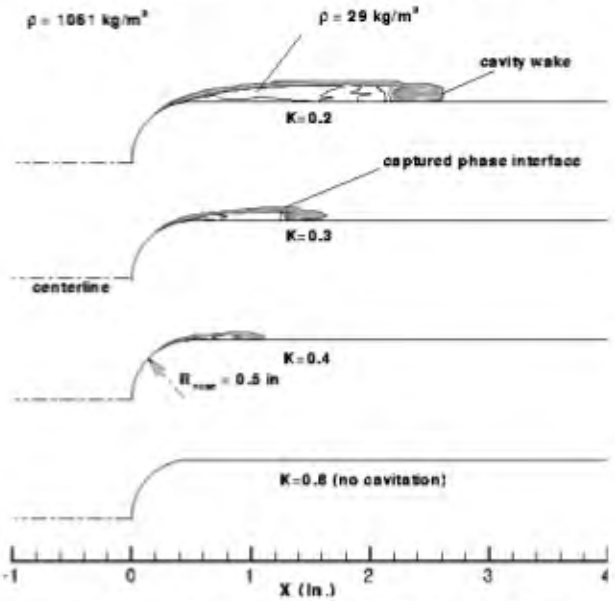

Fig. 12 Density contours of liquid water flow over hemisphere/cylinder for various cavitation numbers. (Ref. 35,36)

The answer to (1), based on my experiences and those reported in the literature, is that it is desirable to have this sort of mechanism, although it may not be absolutely necessary. Thus, question (2) leads to finding an alternative, and the more difficult question (3) will be left alone for now.

In AUSMDV,[1] the convective part of the momentum

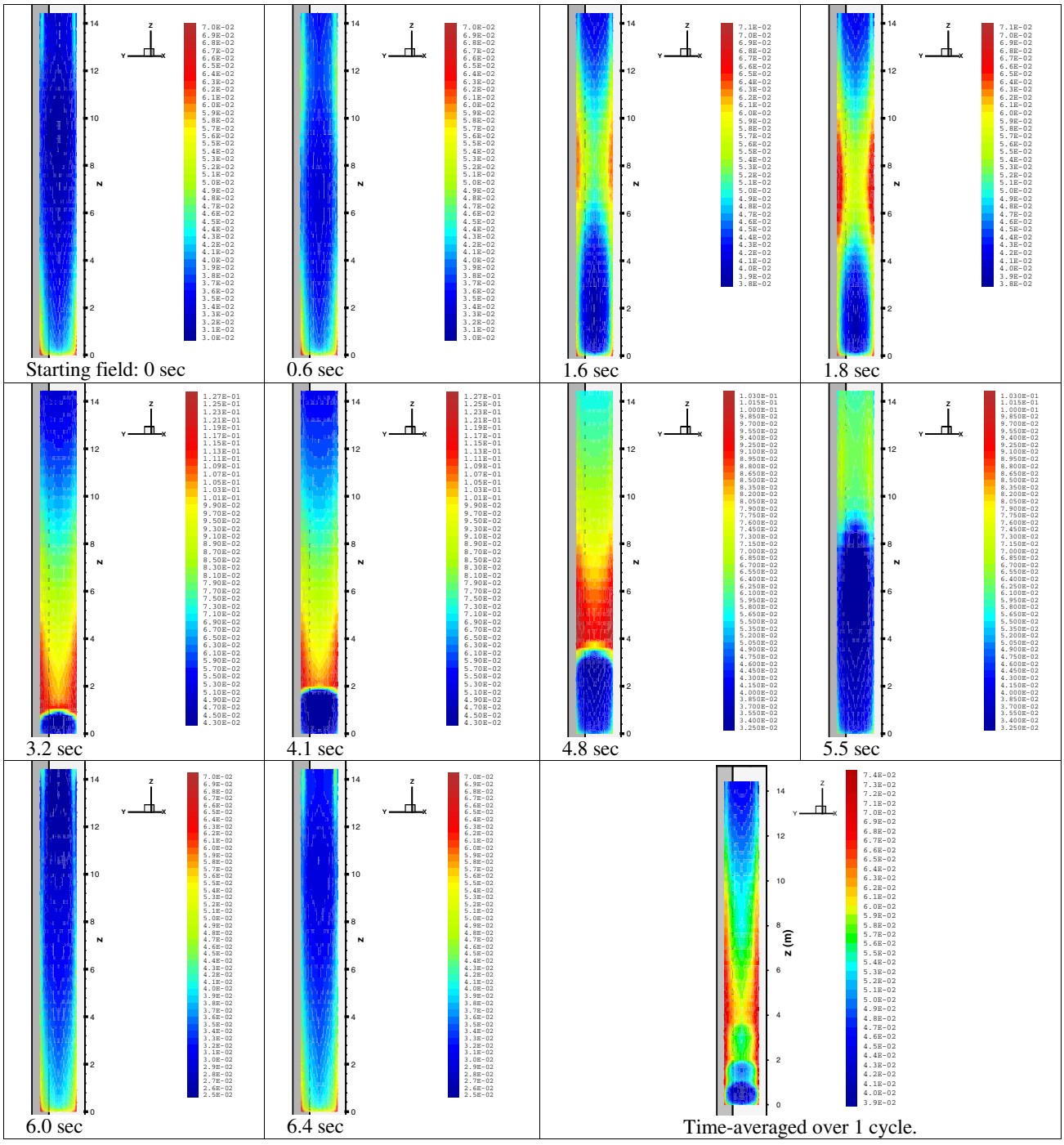

Fig. 14 Time-accurate calculations of the solid volume fractions in an industrial scale riser, with gas and granular particles flowing from the bottom and exiting at the top. (Ref. 17)

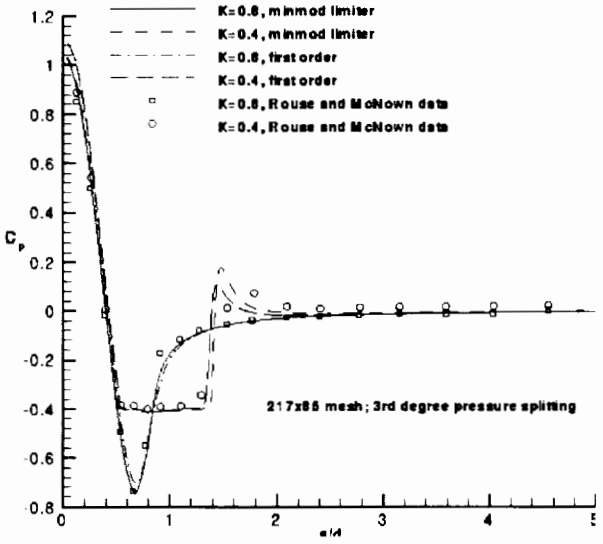

Fig. 13 Effect of spatial discretization accuracy on surface pressure distribution. (Ref. 35, 36)

flux consists of blending the flux-difference and flux-vector procedures (thus denoted with DV). A notable advantage of this strategy is that it gives smooth shock profiles, e.g., in shock-shock interactions. The notion was adopted in the AUSM$^+$-W,[4] but its effectiveness has never been extensively tested. This blended flux can be recast and the extra terms can be reassigned to the pressure flux, giving rise to a new pressure flux containing a term proportional to the velocity difference. This interpretation, however, has a sound connection to the characteristic equations,

$$dp \pm \rho a du = 0, \quad \text{along} \quad \frac{dx}{dt} = u \pm a. \tag{37}$$

An integrated form for the interface pressure for $|u| < a$ is

$$p_{1/2} = \frac{1}{2}[(p_L + p_R) - \rho_{1/2} a_{1/2}(u_R - u_L)]. \tag{38}$$

Hence, we can beef up the pressure flux, Eq. (30) by including the velocity difference term,

$$\begin{aligned} p_{1/2} = \quad & \mathcal{P}^+_{(5)}(M_L)p_L + \mathcal{P}^-_{(5)}(M_R)p_R \\ & -\mathcal{P}^+_{(5)}(M_L)\mathcal{P}^-_{(5)}(M_R)\rho_{1/2}a^2_{1/2}(M_R - M_L), \end{aligned} \tag{39}$$

where for the interface quantity $\rho_{1/2}$ we may use, e.g.,

$$\rho_{1/2} = \begin{cases} (\rho_L + \rho_R)/2 \\ \sqrt{\rho_L \rho_R} \end{cases} \tag{40}$$

The coefficient involving $\mathcal{P}^+_{(5)}(M_L)$ and $\mathcal{P}^-_{(5)}(M_R)$ is introduced to automatically transition between supersonic and subsonic conditions. The pressure now is explicitly coupled with the velocity field by the addition of the velocity difference term. As M tends to zero, the pressure flux reduces to a form similar to Eq. (38), but with half of its coefficient,

$$p_{1/2} = \frac{1}{2}[(p_L + p_R) - \frac{1}{2}\rho_{1/2} a_{1/2}(u_R - u_L)]. \tag{41}$$

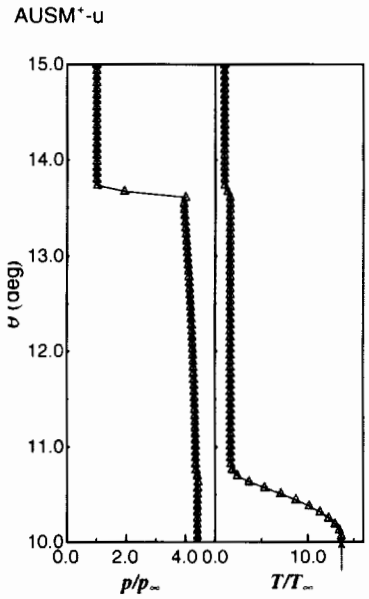

Fig. 15 Hypersonic conic flow.

To denote this new version, we use the suffix "u" (for velocity diffusion) and call it AUSM$^+$-u. Thus, when $\dot{m}_p$[29] is also included, the scheme reads AUSM$^+$-up. Or if the numerical speed of sound is also activated, the version becomes AUSM$^+$-au. Note that if AUSM$^+$-au is used, then the coefficient in Eq. (39) is scaled however, with the numerical speed of sound $\tilde{a}$. This is just what we want for low Mach number flows since $\tilde{a} = O(u)$ as $|u| \to 0$ and hence the coefficient is scaled by the magnitude of local velocity. More details concerning this latest development shall be given in a separate paper.[37]

In what follows we shall consider several benchmark problems I usually used for testing numerical schemes. They represent various facets encountered in typical flow problems. We shall first consider one-dimensional problems and use the first-order scheme.

First, we must require that the new pressure flux be capable of correctly predicting viscous flows, such as the hypersonic conic flow mentioned in the beginning. The new scheme, AUSM$^+$-u, as in the other AUSM-family schemes, gives the correct solution. as seen in Fig. 15. The reason that the velocity difference term does not cause adverse effect is that the velocity components in Eq. (39) are those normal to the cell face and they are continuous across the viscous layer.

The complaint voiced commonly about the AUSM$^+$ concerns the overshoots resulting from strong shock-shock interactions. Figure 16 shows the comparison of results from various schemes. The new pressure flux AUSM$^+$-u now gives a significantly improved result and the AUSM$^+$-up scheme completely removes the overshoots, yielding results as good as those by the AUSMDV, Roe and Godunov schemes. It is a major success since the AUSMDV scheme in

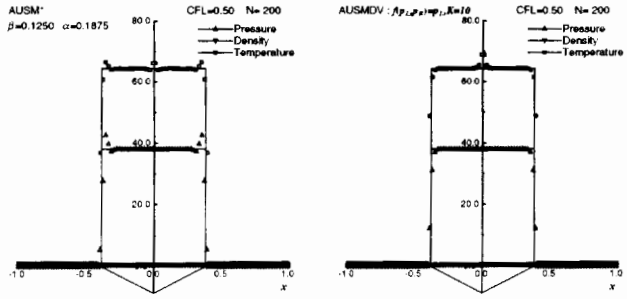

a) AUSM$^+$.

b) AUSMDV.

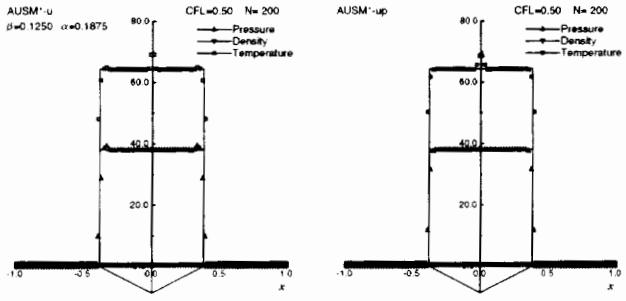

c) New pressure flux, AUSM$^+$-u.

d) AUSM$^+$-up.

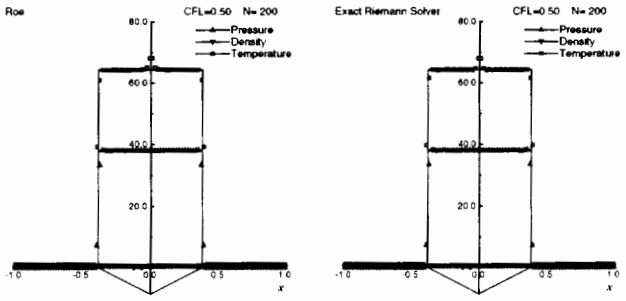

e) Roe's scheme.

f) Godunov's scheme.

Fig. 16 Colliding shock problem

this regard. This test clearly indicates that the new pressure flux formula is a worthy replacement of the old one and will be used again in the following tests.

The second problem concerns a shock moving slowly against a flow, as studied in Ref. 38. Figures 17 shows the strength of linear and nonlinear waves by the AUSM$^+$, AUSM$^+$-u (AUSM$^+$-up is indistinguishable and not shown), Roe, and Godunov schemes. It is known that the Roe and Godunov schemes produces a noticeable long wave trailing the shock, as seen in the figure. The AUSM schemes however, perform quite well.

The third problem is a shock moving through a constant area channel in which the grid at the centerline is perturbed alternately at odd and even points, as proposed by Quirk.[39] Figure 18 displays the result from the new scheme, it like the AUSM$^+$ is clearly free of any shock instabilities.

Next we will consider two two-dimensional supersonic problems using a third-order spatial discretiza-

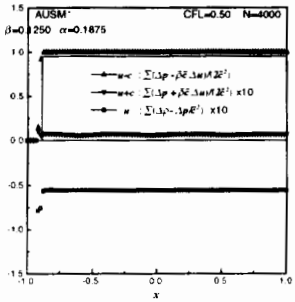

a) AUSM$^+$.

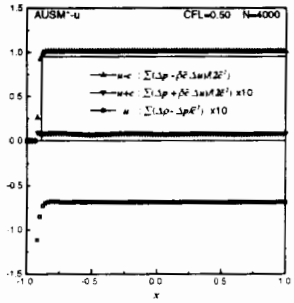

b) New pressure flux, AUSM$^+$-u.

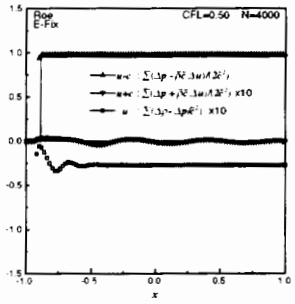

c) Roe's scheme.

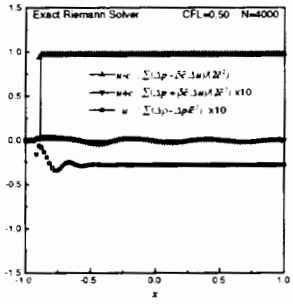

d) Godunov's scheme.

Fig. 17 Slowly moving shock problem.

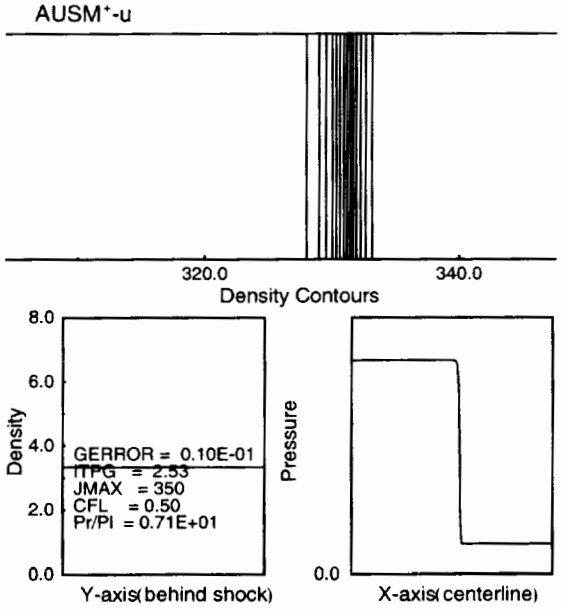

Fig. 18 Odd-even problem.

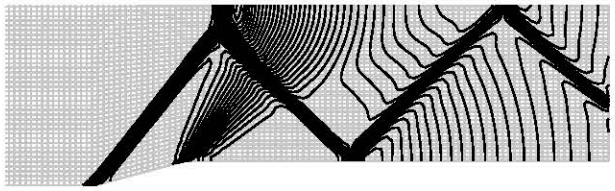

a) Pressure contours:AUSM$^+$-au

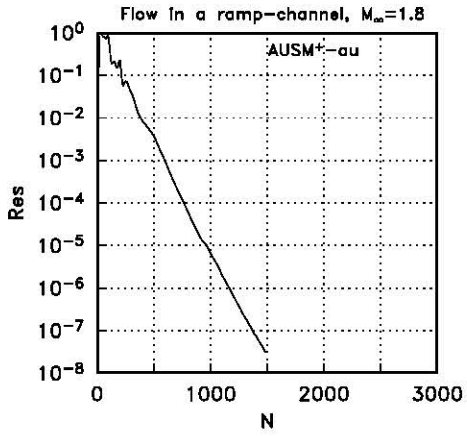

b) Residual history

Fig. 19 Supersonic flow in a ramp-channel, $M_\infty = 1.8$.

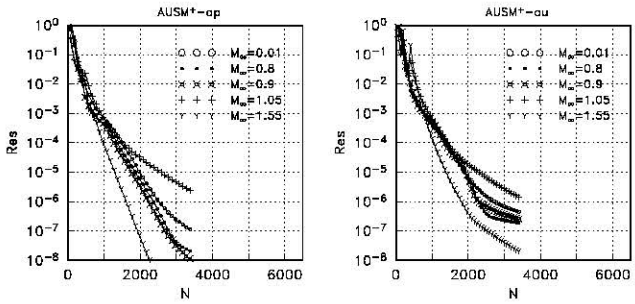

a) AUSM$^+$-ap. b) AUSM$^+$-au.

Fig. 20 Residual history for the shuttle external tank at various Mach numbers.

tion. A supersonic flow in a ramp-channel is shown in Fig. 19. The pressure contours show a smooth behavior across shocks and the residual converges monotonically, again reaffirming the effectiveness of the new pressure flux.

Figures 20 display the comparison of the convergence rates for different flow speeds between the two schemes, AUSM$^+$-ap[29] and the present AUSM$^+$-au. The convergence history by the new pressure flux is essentially the same as the AUSM$^+$-ap scheme up to $N = 2400$, but appears to have slowed down afterward. The reason is not clear and will be further investigated using different codes and for different problems. However, it must be noted that the solutions from these two schemes are not distinguishable.

The final test is a blunt body problem often used by Radespiel.[40] This problem has several features to

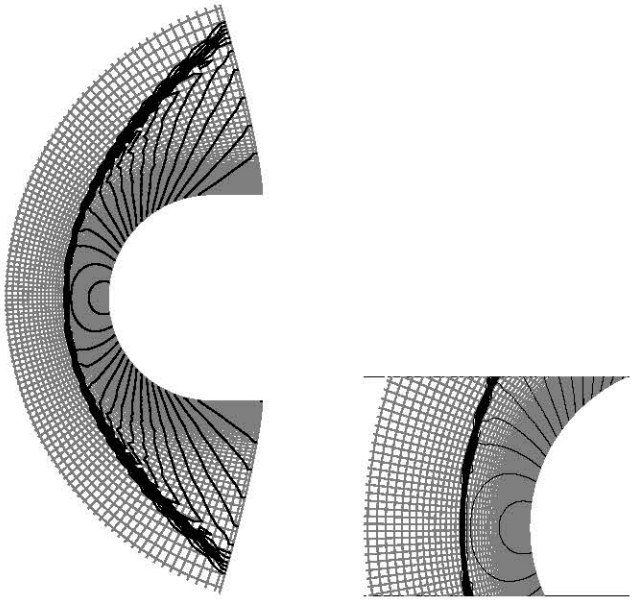

a) New pressure flux, AUSM$^+$-au. b) Blow-up view.

Fig. 21 Blunt body problem, $M_\infty = 10$.

study. The grid[3] is clearly for the viscous calculations, but is tested here for the Euler solutions. First, the solution is free of carbuncle phenomena, consistent with the conjecture given in Ref. 2 since there is no explicit pressure diffusion term in the mass flux. Secondly, the pressure contours are smooth, not only near the wall, shown in the blow-up view near the stagnation region, but also near the sonic line region.

Concluding Remarks

We have just seen a brief history of the AUSM-family, having finished the first ten years from its inception. It has seen both triumphs and setbacks while facing realities and difficult tasks. Nevertheless, many researchers have contributed in different ways towards its growth. The question is whether it will have the longevity to beat the odds in the future, to see a even wilder world. I believe that it has the fundamentally right stuff, even though some turns and twists are expected every time there is a new frontier to be explored. In this brief tour, we have seen the successes, not only in aerodynamics, but also in the areas of DNS/LES and multiphase flows. Furthermore, the new pressure flux boosts the strengths of the AUSM-family, having removed the overshoots behind the shock-shock interactions–a major success since the AUSMDV scheme in this regard. These should give us sufficient confidence in its ability to provide needed accuracy, efficiency, and robustness.

[3]The grid was provided by Prof. Rolf Radespiel, Braunschweig Technical University, Germany.

References

[1]Wada, Y. and Liou, M.-S., "An accurate and robust flux splitting scheme for shock and contact discontinuities," *SIAM Journal on Scientific and Statistical Computing*, Vol. 18, 1997, pp. 633–657.

[2]Liou, M.-S., "Mass flux Schemes and connection to shock instability," *Journal of Computational Physics*, Vol. 160, 2000, pp. 623–648.

[3]Liou, M.-S. and Steffen, Jr., C. J., "A new flux splitting scheme," *Journal of Computational Physics*, Vol. 107, 1993, pp. 23–39, Also NASA TM 104404, May 1991.

[4]Liou, M.-S., "Progress towards an improved CFD method: AUSM$^+$," AIAA Paper 95-1701-CP, 12th AIAA CFD Conference, 1995.

[5]Radespiel, R. and Kroll, N., "Accurate flux vector splitting for shocks and shear layers," *Journal of Computational Physics*, Vol. 121, 1995.

[6]Liou, M.-S., "A sequel to AUSM: AUSM$^+$," *Journal of Computational Physics*, Vol. 129, 1996, pp. 364–382, Also NASA TM 106524, March 1994.

[7]Shima, E. and Jounouchi, T., "AUSM Type Upwind Schemes," 1994, (in Japanese).

[8]Edwards, J. R., "A low-diffusion flux-splitting scheme for Navier-Stokes calculations," *Computers & Fluids*, Vol. 26, 1997, pp. 635–659.

[9]Kim, K. H., Lee, J. H., and Rho, O. H., "An improvement of AUSM schemes by introducing the pressure-based weight functions," *Computers and Fluids*, Vol. 27, 1998, pp. 311–346.

[10]Moschetta, J.-M. and Gressier, J., "The sonic point glitch problem: a numerical solution," *Lecture Notes in Physics, Volume 515*, 1998, pp. 403–408.

[11]Stewart, H. B. and Wendroff, B., "Two-phase flow: models and methods," .

[12]Toumi, I., Kumbaro, A., and Paillère, H., "Approximate Riemann solvers and flux vector splitting schemes for two-phase flow," VKI Lecture Series 1999-03, 30th Computational Fluid Dynamics, von Karmann Institute, Belgium, 1999.

[13]Turkel, E., "Preconditioned methods for solving incompressible and low speed compressible equations," *Journal of Computational Physics*, Vol. 72, 1987, pp. 277–298.

[14]van Leer, B., Lee, W. T., and Roe, P. L., "Characteristic time stepping or local preconditioning of the Euler equations," AIAA Paper 91-1552, July 1991.

[15]Choi, Y. H. and Merkle, C. L., "The application of preconditioning in viscous flows," *Journal of Computational Physics*, Vol. 105, 1993, pp. 207–223.

[16]Weiss, J. M. and Smith, W. A., "Preconditioning applied to variable and constant density time-accurate flows on unstructured meshes," AIAA Paper 94-2209, June 1994.

[17]De Wilde, J., Vierendeels, J., and Dick, E., "An extension of the preconditioned AUSM to two-phase flows for the 3D calculations of circulating fluidized beds," *Third Intern. Symposium on Computational Technologies for Fluid/Thermal/Chemical Systems with Applications, ASME-PVP*, 2001.

[18]van Leer, B., Thomas, J. L., Roe, P. L., and Newsome, R. W., "A comparison of numerical flux formulas for the Euler and Navier-Stokes equations," AIAA Paper 87-1104CP, 8th AIAA CFD Conference, 1987.

[19]Hänel, D. and Schwane, R., "An Implicit Flux-Vector Splitting Scheme for the Computation of Viscous Hypersonic Flow," AIAA Paper 89-0274, 1989.

[20]Liou, M.-S. and Steffen, Jr., C. J., "Development of a new flux splitting scheme," , No. 91-11611-CP (open forum), June 1991, pp. 967–968.

[21]Godunov, S. K., "A Difference Method for the Numerical Calculation of Discontinuous Solutions of Hydrodynamic Equations," *Mat. Sb.*, Vol. 47, 1959, pp. 271–306, translation, US JPRS: 7225, November, 1960.

[22]Halt, D. W. and Agarwal, R. K., "A novel algorithm for the solution of compressible Euler equations in wave/particle split (WPS) form," Open forum paper, 11th AIAA CFD Conference, 1993.

[23]Darracq, D., Champagneux, S., and Corjon, A., "Computation of unsteady turbulent airfoil flows with an aeroelastic AUSM$^+$ implicit solver," AIAA Paper 98-2411, 1998.

[24]Cook, P. H., McDonald, M. A., and Firmin, M. C. P., AGARD Report 138, 1979.

[25]Billet, G. and Louedin, O., "Adaptive limiters to improve the accuracy of MUSCL approach for unsteady flows," *Journal of Computational Physics*, to appear.

[26]Meinke, M., Rister, T. R., Rütten, F., and Schvorak, A., "Simulation of internal and free turbulent flows," *Lecture Notes in Physics, Volume 515*, 1998, pp. 201–206.

[27]Louedin, O. and billet, G., "Study of turbulence modeling for transient high speed flow with 2D and 3D large eddy simulation based on temporal filter," *First AFOSR International Conference on DNS/LES*, Ruston, Louisiana, August 1997.

[28]Dailey, L. D. and Pletcher, R. H., "Evaluation of a second-order accurate compressible finite volume formulation for the large eddy simulation of turbulent flows," *First AFOSR International Conference on DNS/LES*, Ruston, Louisiana, August 1997.

[29]Liou, M.-S. and Edwards, J. R., "Numerical speed of sound and Its application to schemes for all speeds," AIAA Paper 99-3268-CP, 14th AIAA CFD Conference, 1999.

[30]Mary, I., Sagaut, P., and Deville, M., "An algorithm for unsteady viscous flows at all speeds," *International Journal for Numerical Methods in Fluids*, Vol. 34, 2000, pp. 371–401.

[31]Buning, P. G. and et. al., "OVERFLOW user's manual, version 1.8f," Unpublished NASA Report, 1998.

[32]Liou, M.-S. and Rogers, S. E., "Calculations of low speed flows over a high-lift configurations using the AUSM$^+$-ap scheme," (in preparation).

[33]Spalart, P. R. and Allmaras, S. R., "A one-equation turbulence model for aerodynamic flows," AIAA Paper 92-0439, 1992.

[34]Paillère, H., Core, C., and Garcia, J., "On the extension of the AUSM$^+$ scheme to compressible two-fluid models," to appear (2001).

[35]Liou, M.-S. and Edwards, J. R., "AUSM schemes and extensions for low Mach and multiphase flows," VKI lecture series 1999-03, VKI, Belgium, 1999.

[36]Edwards, J. R., Franklin, R. K., and Liou, M.-S., "Low-diffusion flux-splitting methods for real fluid flows at all speeds," *AIAA Journal*, 2000.

[37]Liou, M.-S., "to be determined," (in preparation).

[38]Roberts, T. W., "The Behavior of Flux Difference Splitting Schemes near Slowly Moving Shock Waves," *Journal of Computational Physics*, Vol. 90, 1990, pp. 141–160.

[39]Quirk, J. J., "A Contribution to the Great Riemann Solver Debate," *Int. J. Numer. Methods Fluids*, Vol. 18, 1994, pp. 555–574, Also ICASE Report 92-64, 1992.

[40]Radespiel, R., "Efficient computation of compressible flows," *Lecture Notes in Physics*, Vol. 515, 1998, pp. 237–253.

REPORT DOCUMENTATION PAGE

Form Approved
OMB No. 0704-0188

1. AGENCY USE ONLY (*Leave blank*)	2. REPORT DATE	3. REPORT TYPE AND DATES COVERED
	November 2001	Technical Memorandum

4. TITLE AND SUBTITLE

Ten Years in the Making—AUSM-family

5. FUNDING NUMBERS

WU–708–28–13–00

6. AUTHOR(S)

Meng-Sing Liou

7. PERFORMING ORGANIZATION NAME(S) AND ADDRESS(ES)

National Aeronautics and Space Administration
John H. Glenn Research Center at Lewis Field
Cleveland, Ohio 44135–3191

8. PERFORMING ORGANIZATION REPORT NUMBER

E–12831

9. SPONSORING/MONITORING AGENCY NAME(S) AND ADDRESS(ES)

National Aeronautics and Space Administration
Washington, DC 20546–0001

10. SPONSORING/MONITORING AGENCY REPORT NUMBER

NASA TM—2001-210977
AIAA–2001–2521

11. SUPPLEMENTARY NOTES

Prepared for the 15th Computational Fluid Dynamics Conference sponsored by the American Institute of Aeronautics and Astronautics, Anaheim, California, June 11–14, 2001. Responsible person, Meng-Sing Liou, organization code 5880, 216–433–5855.

12a. DISTRIBUTION/AVAILABILITY STATEMENT

Unclassified - Unlimited
Subject Categories: 02 and 34 Distribution: Nonstandard

Available electronically at http://gltrs.grc.nasa.gov/GLTRS
This publication is available from the NASA Center for AeroSpace Information, 301–621–0390.

12b. DISTRIBUTION CODE

13. ABSTRACT ***(Maximum 200 words)***

We begin by describing the motivations that gave birth to the original AUSM scheme and then focus on the ingredients that has spurred its growth and acceptance by the world of computational fluid dynamics. As it has played out more in the field, weaknesses have also surfaced. Hence, nutrients and supplements are prescribed to help it grow and stay strong and robust. In this paper, we will describe the saga of efforts owing to researchers who have contributed to building up the AUSM-family for the CFD community. It is hoped that a healthy scheme will contribute to the accurate and robust solution of problems encountered in a wide range of disciplines. We analyze numerical mass fluxes with an emphasis on their capability for accurately capturing shock and contact discontinuities. We will present a new scheme for the pressure flux, along with results for a host of test problems.

14. SUBJECT TERMS	15. NUMBER OF PAGES
CFD; Upwind schemes; AUSM schemes; Low Mach-number flows; Multiphase flows	21
	16. PRICE CODE

17. SECURITY CLASSIFICATION OF REPORT	18. SECURITY CLASSIFICATION OF THIS PAGE	19. SECURITY CLASSIFICATION OF ABSTRACT	20. LIMITATION OF ABSTRACT
Unclassified	Unclassified	Unclassified	